Bioinspired Universal Flexible Elastomer-Based Microchannels

The Harvard community has made this article openly available. **Please share** how this access benefits you. Your story matters

Citation	Wu, Feng, Songyue Chen, Baiyi Chen, Miao Wang, Lingli Min, Jack Alvarenga, Jie Ju, et al. 2018. "Bioinspired Universal Flexible Elastomer-Based Microchannels." Small 14 (18) (January 11): 1702170. doi:10.1002/smll.201702170.
Published Version	doi:10.1002/smll.201702170
Citable link	http://nrs.harvard.edu/urn-3:HUL.InstRepos:37235081
Terms of Use	This article was downloaded from Harvard University's DASH repository, and is made available under the terms and conditions applicable to Open Access Policy Articles, as set forth at http://nrs.harvard.edu/urn-3:HUL.InstRepos:dash.current.terms-of-use#OAP

WILEY-VCH

4   Bioinspired Universal Flexible Elastomer-Based Microchannels

5   *Feng Wu, Songyue Chen, Baiyi Chen, Miao Wang, Lingli Min, Jack Alvarenga, Jie Ju, Ali Khademhosseini,*

6   *Yuxing Yao, Yu Shrike Zhang, Joanna Aizenberg, and Xu Hou**

7

8   F. Wu, Dr. M. Wang, Prof. X. Hou

9   Bionic and Soft Matter Research Institute, College of Physical Science and Technology

10   Xiamen University

11   361005, Xiamen, China

12   E-mail: houx@xmu.edu.cn

13   Prof. S. Chen

14   Department of Mechanical and Electrical Engineering

15   Xiamen University

16   361005, Xiamen, China

17   Dr. B. Chen, Dr. L. Min, Prof. X. Hou

18   College of Chemistry and Chemical Engineering, and Collaborative Innovation Center of Chemistry for Energy

19   Materials, and State Key Laboratory of Physical Chemistry of Solid Surfaces, and Pen-Tung Sah Institute of Micro-

20   Nano Science and Technology

21   Xiamen University

22   361005, Xiamen, China

23   Dr. J. Alvarenga, Dr. Y. S. Zhang, Prof. A. Khademhosseini, Prof. J. Aizenberg

24   Wyss Institute for Biologically Inspired Engineering

25   Harvard University

26   MA 02138, Cambridge, USA

27   Dr. J. Ju, Dr. Y. S. Zhang, Prof. A. Khademhosseini

28   Biomaterials Innovation Research Center, Division of Engineering in Medicine, Department of Medicine, Brigham

29   and Women's Hospital

30   Harvard Medical School

31   MA 02139, Cambridge, USA

32   Y. Yao, Prof. J. Aizenberg

33   Department of Chemistry & Chemical Biology

34   Harvard University

35   MA 02138, Cambridge, USA

36

37

38

1   Flexible and stretchable microscale fluidic devices have a broad range of potential

2   applications, ranging from electronic wearable devices for convenient digital lifestyle to

3   biomedical devices. However, simple ways to achieve stable flexible and stretchable fluidic

4   microchannels with dynamic liquid transport have been challenging because every

5   application for elastomeric microchannels is restricted by their complex fabrication

6   process and limited material selection. Here we show a universal strategy for building

7   microfluidic devices that possess exceptionally stable and stretching properties. The

8   devices exhibit superior mechanical deformability, including high strain (967%) and

9   recovery ability, where applications as both strain sensor and pressure-flow regulating

10   device are demonstrated. Various microchannels are combined with organic, inorganic,

11   and metallic materials as stable composite microfluidics. Furthermore, with surface

12   chemical modification these stretchable microfluidic devices can also obtain anti-fouling

13   property to suit for a broad range of industrial and biomedical applications.

14   Keywords: Bioinspired, Flexible, Elastomer, Microchannels

15

16

17

18

19

1. Introduction

Advances in microfluidics are revolutionizing many traditional disciplines, such as materials science,[1-4] molecular biology,[5-7] cellular biology,[8-12] drug screening,[3, 13-17] and medical diagnostics.[18] Elastomeric microfluidics with rapid development in recent years has shown exciting potential from wearable electronic devices[19-22] for convenient digital lifestyle to biomedical devices[22-24] that make conformal interfaces with the skin and internal organs. However their broad applications have been significantly restricted by the complex fabrication process[25, 26] and the limited material selection.[27-29] For example, Ziegler et al. showed a classic and reproducible method to realize the fabrication of elastomeric microfluidics by micro-molding and thermal bonding of Parylene.[28] Compared to the general fabrication method, where a sacrificial photoresist layer is sandwiched between two Parylene layers, the poisonous and high-residue photoresist dissolution step is omitted, and the adhesion between the elastomeric Parylene layers is improved. Nevertheless, the micro-molding technique is complicated and expensive, which is difficult to adapt to industry requirements at present. In addition, Ota et al. developed a platform to conveniently fabricate liquid-liquid 'heterojunction' devices for the use as liquid-state electronic elastomeric systems.[27] But this method has been significantly limited by its circumscribed material selection. Moreover, the inner surface of these microchannels are easily contaminated due to the strong adsorption of molecules onto these bulk materials.[30, 31] The above-

1 mentioned issues have largely affected the development of the conventional elastomeric

2 microfluidic devices and their applications in various fields, such as wearable electronic

3 devices,[1, 19-22] biomolecule separation,[32, 33] and anti-fouling technology.[30, 31]

4 To overcome above challenges, various strategies have been proposed to prepare

5 elastomeric microchannel (EM). Yuk et al. reported a method to assemble hydrogels

6 and elastomers into hybrids with robust interface and functional microstructures, such

7 as microchannels and electrical circuits inside hydrogels.[34] They used the double-sided

8 acrylic tape elastomers which are made of mixtures of aliphatic acrylate photocured

9 during the film processing (3M VHB membranes) as the good packaging material to

10 seal the hydrogel. Besides, Kubo et al. described a strategy for fabricating the

11 stretchable and mechanically stable radiofrequency antenna, which consisted of liquid

12 metal enclosed in the elastomeric microfluidic channels.[35] Its high stretchability

13 allowed its resonance to be mechanically tuned over a wide range of frequencies. To

14 date, most of the elastomeric microfluidics works under the conditions of the liquid is

15 enclosed inside the channels without the flowing. Building elastomeric microfluidics

16 with controllable channel sizes and dynamic flowing is still challenging due to material

17 selection limitation, lack of simple and general fabrication process, and fouling issue,

18 but has a great potential applications, such as soft robotics[36] and tissue engineering.[37]

19 To address above issues, here we report a universal strategy to build bioinspired

20 flexible elastomer-based microchannel systems with controllable channel sizes, which

1   show extraordinarily stable and stretchable properties for many potential applications

2   such as the strain sensor and the pressure-flow regulating device. Though showing the

3   excellent flexibility and high adhesion, 3M VHB membrane has been applied in the

4   large research and industrial communities only as the adhesive tapes. Here we used 3M

5   VHB membranes, not only as the good packaging material, but also as the important

6   substrate for directly preparing the microchannels. And our microchannel fabrication is

7   compatible with many existing techniques, such as laser cutting,[38] blade cutting,[39]

8   photolithography,[40] and thermo-molding,[41] and is also easily scalable for the large-

9   scale fabrication. These stable elastomer-based microchannels not only exhibit

10   excellent flexible and stretchable characteristics, but also can show the good anti-

11   fouling property by further chemical modification of the inner surface of the channels.

12   Such an universal approach for making dynamic microfluidics can potentially serve as

13   a new platform with broad applications.[1]

14

15   **2.   Results and discussion**

16   **2.1. Multi-dimensional microchannels with controllable sizes**

17   Blood vessels in living organisms have multi-dimensional channels structures, with

18   flexibility and stretchability.[42, 43] Inspired by blood vessels, the multi-dimensional (1D,

19   2D and 3D) microchannels were fabricated to show the flexible and stretchable

20   properties (**Figure 1a**). For 1D, the EM possessed excellent flexibility, and allowed the

1 liquid flow inside the channel without any leakage even in a large-scale curve. For 2D,

2 the EM patterned in alphabetic letters would be easily prepared by utilizing the laser

3 cutting method (Figure 1a bottom left and Figure S1, Supporting Information). These

4 microchannels could be homogeneously fabricated, with size easily tuned by the laser

5 power and the engraving time (Table S1 and Figure S2, S3, Supporting Information).

6 For 3D, the elastomer-based microchannels could be obtained by the stacking method,

7 and tested with the external force applied. It showed the excellent sealability after

8 stretching and releasing (Figure 1a bottom right and Video S1, Supporting Information).

9 The size of blood vessels in living organisms are controllable by blood pressure to

10 maintain normal metabolism.[44, 45] Our bioinspired microchannels could also regulate

11 the channel size by controlling the flow pressure (Figure 1b).
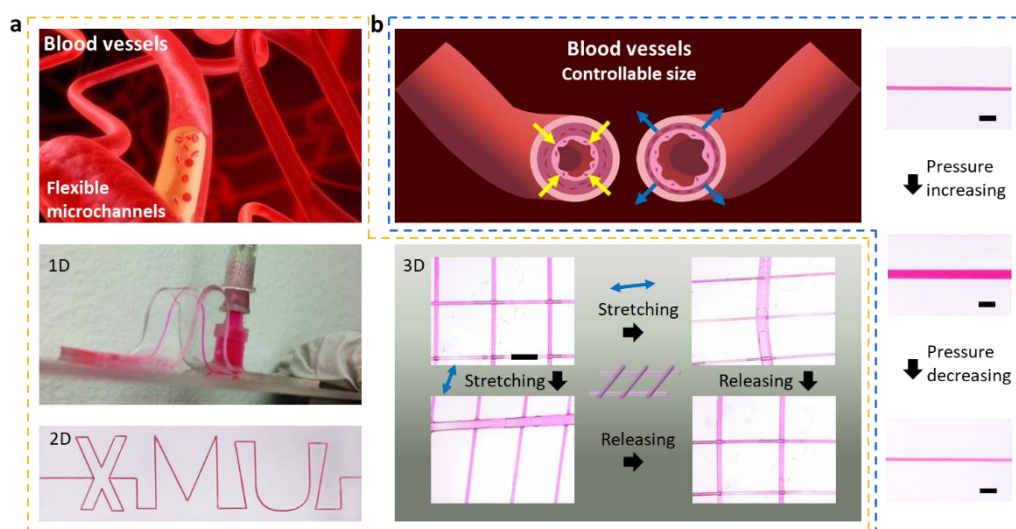

12

13 **Figure 1.** a) Bioinspired flexible microchannels. Flexible blood vessels (Top left). 1D flexible

14 elastomer-based microchannel (Middle left), 2D elastomer-based microchannel with the letter

pattern (Bottom left), and 3D elastomer-based microchannels with stretchable and reversible properties (Bottom right). b) Bioinspired microchannels with controllable sizes. Blood vessels with tunable sizes (Top left). The size changes of the elastomer-based microchannel by regulating the flowing pressure (Right). Scale bars, 2 mm.

2.2. Tensile property

One particularity of elastomer-based microchannels originates from its super-elastic property. To further explore the mechanical property, tensile test was performed in comparison with the standard polydimethylsiloxane (PDMS) microchannel, as shown in **Figure 2a**. With the difference from PDMS, the EM sustained continuous spreading and demonstrated the superior stretchability, as well as the elastic-strain recovery ability after releasing (Video S2, Supporting Information). The stress-strain curves of both materials are shown in Figure 2b. The elongation of the EM at break reached 967 ± 40%, compared with 368 ± 31% for that of PDMS. The Young's modulus of the EM calculated at linear deformation region reaches ~60 kPa, which is a rather low value even for the elastic polymer materials.
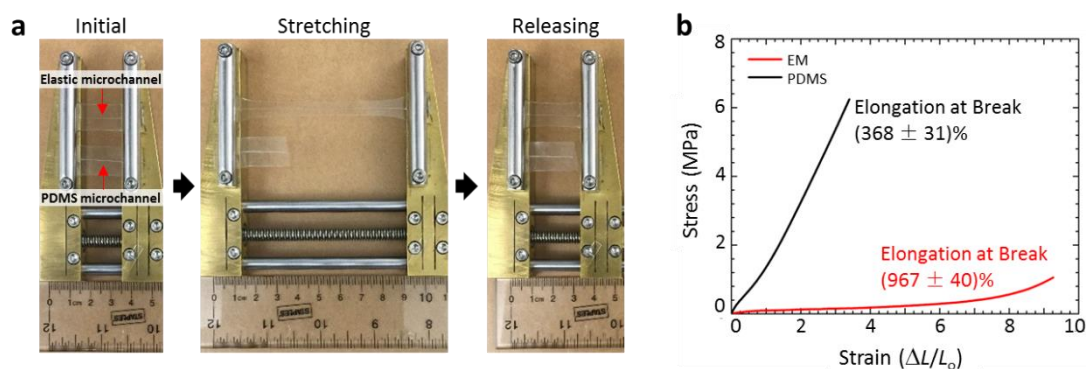
Figure 2. The mechanical property of the elastomeric stretchable microchannel. a) Comparative experiment between the EM and PDMS-based microchannel. b) Stress-strain curves of the EM and PDMS.

2.3. Application as a strain sensor

A strain gauge was designed for the sensitive force sensing based on the outstanding mechanical property of the EM at small forces, as shown in **Figure 3a**. Resistance change of microchannel was measured under different tension. The microchannel was filled with 0.1 M KCl as the ionic conductor, and the current was measured by applying 0.1 V to two Ag/AgCl electrodes inserted into both the inlet and outlet. The ionic conductor in this microchannel served as the deformable interconnections without the risk of cracking as is the concern for metal interconnections.[46, 47] The normalized resistance change $\Delta R/R$ is a function of strain s:

$$\frac{\Delta R}{R} = \frac{1+s}{(1-vs)^2} - 1,$$

where $s = \Delta L/L_{o}$, and v represents the Poisson's ratio for the microchannel. Figure 3b shows the normalized resistance change with respect to stress. The corresponding real-

1   time current change measurement is shown in Figure S4a. The measured Poisson's ratio

2   of EM took the value of ~0.15, while the fitting curve (Figure 3b inset) with the

3   experimental data of *v* for the microchannel was 0.093, indicating that compared with

4   the bulk material, the microchannel has less transversal dimension change when being

5   stretched. The strain gauge possesses a force sensitivity of $6\Delta R/R$ per Newton. Another

6   potential advantage of the EM over PDMS for application in sensing lies in that the gas

7   impermeability of the EM allows long-term chemical stability for the liquid filled inside

8   the channel.[48, 49]
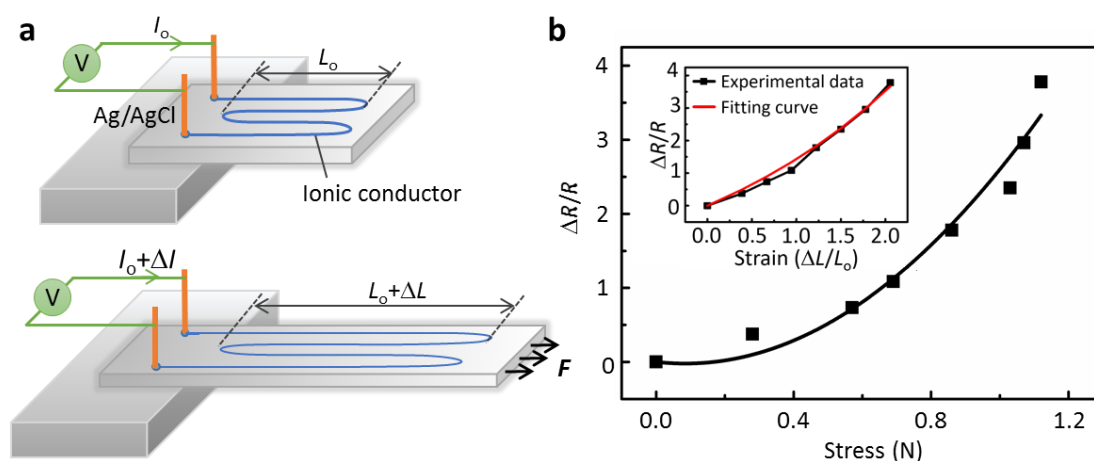
9   **Figure 3.** a) Strain gauge based on the EM and the ionic conductor. b) Resistance change curve with
10   the different stress, where the inset is the normalized resistance change with the different strain.

11   **2.4. Lateral deformability**

12   Besides the longitude deformability, the fabricated microchannel device also showed

13   the lateral deformability. The shape of the channel's cross-section was recorded upon

14   stretching the device and releasing. As shown in **Figure 4a**, the six-colored channels of

1   triangular shape were discretely distributed. It should be noted that, there was no liquid

2   inside the microchannels when we obtained the images of the cross-section of these

3   channels. Before we obtained these images, the inner wall of these microchannels had

4   been dyed with the Rhodamine B solution, and then we dried it to obtain a clear contour

5   of the channels when taking the images during its deformation. By applying an in-plane

6   force perpendicular to the channels, the initial triangular channels completely closed

7   and the section thickness decreased. After releasing the force, this highly compressed

8   state completely recovered and the channels opened again owning to the excellent

9   elastic property of EM.

10   The force-sensitive deforming feature of this elastomer-based microfluidic device

11   showed great potential in the application of force/pressure regulation. Figure 4b has

12   provided a simple illustration of such application. A syringe pump was used here to

13   supply continuous fluid at a constant flow rate Q (300 µL min^{-1}) into a single-channeled

14   microfluidic device and a digital cantilever capable of supplying small amount of force

15   was harnessed to exert force to the upper surface of the microchannel. A highly sensitive

16   pressure gauge connected near the inlet and outlet of the channel was used to monitor

17   the real-time pressure change. The pressure drop $\Delta P = Q \cdot R_{hyd}$, where flow rate $Q \approx$

18     $v_s \cdot w \cdot h$, the hydraulic resistance $R_{hyd} \approx \alpha \mu L / w h^3$, and v_s denotes the fluid velocity, μ the

19   viscosity of the fluid, L, w, and h the length, width and height of the channel for the

20   rectangular cross-section, respectively, and α the constant related to the shape of the

cross-section.[50, 51] Therefore, for the constant flow rate in our case, ΔP is inversely proportional to h^2. The cross-section size reduced by pressing on the microchannel, causing the increase of the hydraulic resistance and finally pressure boosting.

Specific to the experiment, the initial size of the channel without any pressure was ~250 μm in width, and ~400 μm in height and the velocity of water was set to be 300 μL min^{-1}. In the first 200 s, the pressure was building up to a relatively stable value of 13 kPa without external force to the upper surface. At 400 s, the force of 0.2 N was exerted to the exterior surface of the channel, ΔP increased accordingly and stabilized at about 11.3 kPa at 600 s. After that, the force was elevated to 0.6 N, and ΔP underwent another climbing to 18 kPa at 1000 s. For a microfluidic system with fixed diameter and inner fluid velocity, the force can be detected by using the force-pressure drop calibration curve, indicating a potential application for the pressure sensor system.
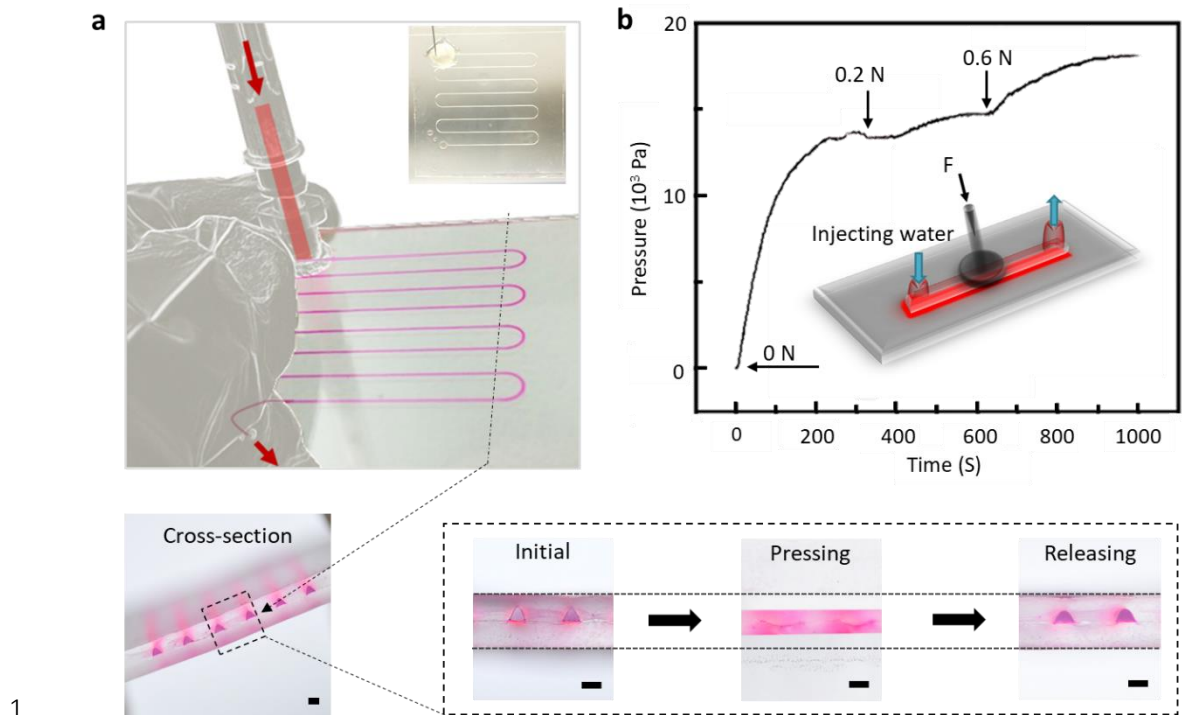
Figure 4. The elastomer-based microchannel's application as a pressure sensor. a) The compressible microchannels and its excellent recovery property. After crosscutting, separated microchannels can be observed clearly. By applying a force perpendicular to the channels, the initial triangular microchannels completely closed and the section thickness decreased. After releasing, the closed microchannels fully recovered again. Inset image shows a clear microfluidics before injection. b) Applied forces can be reflected by the variation of the transfer liquid pressure inside the microchannel. Scale bars, 400 μm.

2.5. Adhesion to various materials

Another superiority of this microfluidics was its vast applicability on various substrates directly, without any surface modifications. As illustrated in **Figure 5**, due to its intrinsic adhesive property, the EM could be transferred on various substrates, including

1   organic (polyethylene terephthalate (PET), polytetrafluoroethylene (PTFE), PDMS,

2   and polymethyl methacrylate (PMMA)), inorganic (glass), and metallic materials. The

3   EM adhered firmly onto different types of substrates, and did not show any leakage

4   from the magnified images. For the metal EM, the seal of the channel was intact even

5   after severe bending. The 90°-peeling test and the liquid-leakage critical pressure

6   measurement also showed good sealing property (Figure S5, Supporting Information).
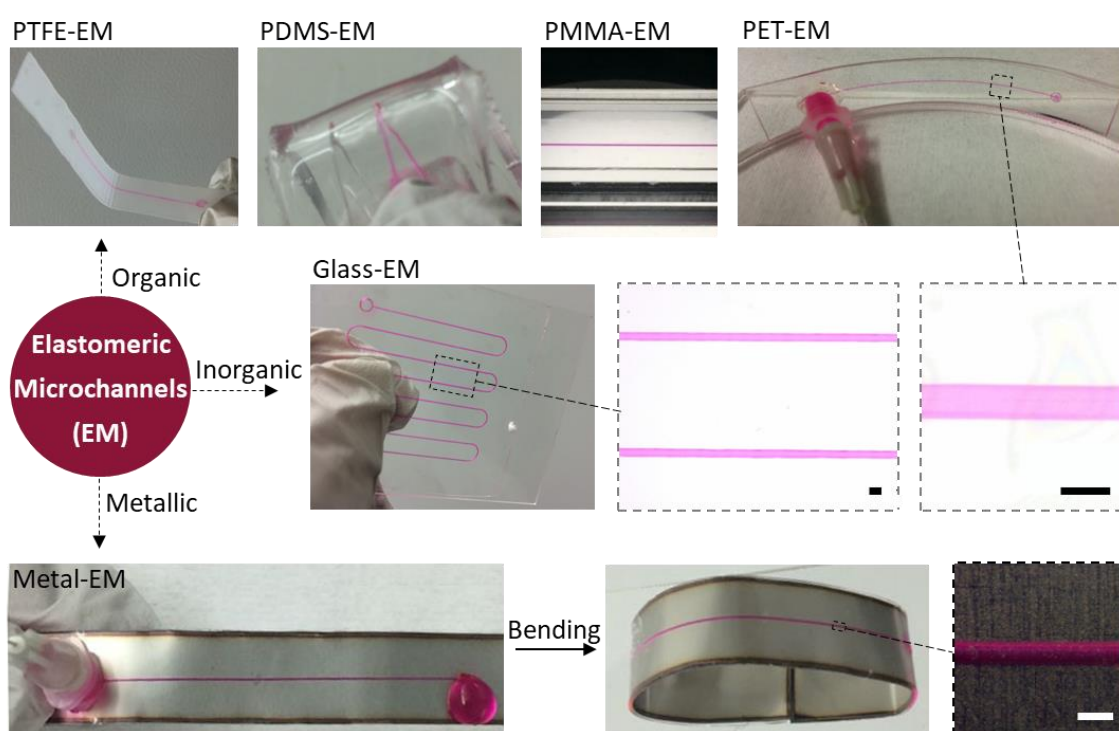
7

8   **Figure 5.** The composite microfluidics prepared by combining the EM with the organic polymeric

9   substrates, the inorganic glass substrate, and the metallic substrate. Scale bars, 200 μm.

10   **2.6. Surface modification for anti-fouling**

11   Fouling is a daunting issue[30] and restricts practical applications of microfluidic

12   channels. To avoid fouling, we modified the inner surface of the microchannel with the

1   amphiphobic agent 1H,1H,2H,2H-Perfluorodecyltrimethoxysilane (PFTS) by using the

2   chemical vapor deposition method. As can be observed in **Figure 6**, the evident changes

3   in the wettability and the anti-fouling capacity of the EM occurred in the process of

4   modification. In Figure 6a, water and dimethylsilicone oil were tested as representative

5   chemicals, where the contact angle analysis was used to test the modification. The inner

6   surface of the microchannel without any treatment showed the contact angles of 82.3°

7   to water droplet and 9.7° to dimethylsilicone oil, respectively, indicating an

8   amphipathicity of the EM. However, after modification by PFTS, the remarkable

9   changes took place in the wettability of the EM surface. As shown in Figure 6a, the

10   intrinsic hydrophilicity transformed into hydrophobic (the contact angle of water

11   increased from 82.3° to 118.8°) and the contact angle of dimethylsilicone oil

12   significantly increased from 9.7° to 72.2°. Meanwhile, the PFTS coating exhibited an

13   excellent anti-fouling capacity. As shown in Figure 6b, the modified microchannel inner

14   surface could completely recover to its initial state without any residue of Rhodamine

15   B, while the microchannel without modification showed the serious contamination with

16   the dye molecules. It should be noted that, the surface could also be modified with many

17   other different method to suite different applications, such as the liquid phase

18   deposition[52] and the chemical composition.[53]
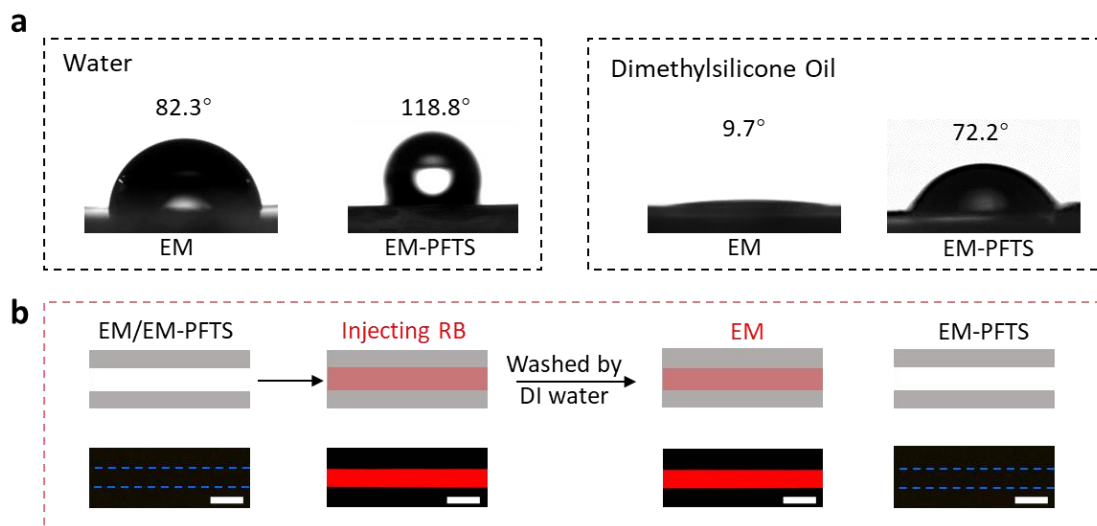
Figure 6. Surface modification of the microchannel inner surface for anti-fouling. a) Water and dimethylsilicone oil contact angle analysis. b) Schematic illustrations (top) and microscopic images of microchannels (bottom). Anti-fouling measurement before and after the surface modification with PFTS on the microchannel inner surface. Scale bars, 50 μm.

3. Conclusion

In summary, we have demonstrated a convenient method to fabricate the elastomer-based microchannel, which possesses the excellent elastic property and dynamic stability with maintaining liquid flows during the stretching and releasing state. Meanwhile, the flexible microchannel can be directly assembled onto various substrates, including organic, inorganic, and metallic. Besides, its inner surface can be conveniently modified by a simple chemical vapor deposition method for anti-fouling application. In addition, the elastomer-based microchannel exhibits excellent mechanical deformability upon stretching (967%) and compressing. Meanwhile, its sensitive deformability upon micro-forces, including both in longitude and lateral

1   directions, shows great potential in the application for strain sensors and pressure

2   sensors.

3   **4. Experimental Section.**

4   For the microchannels materials, the elastomer (VHB 4910, 3M Company) and PDMS

5   (Sylgard 184, Dow Corning Corporation) with the ratio of base: crosslinker 10: 1 were

6   used. To prevent fouling, PTFE (J&K Chemicals, 227930) was used to modify the

7   microchannel inner surface. Both the deionized water (resistivity18.3 MΩ cm) and the

8   dimethylsilicone oil (Macklin, D806810) were used to characterize the wetting

9   behavior of the material surface. KCl (Sinopharm, 10016308) was used to act as the

10   ionic conductor. For the anti-fouling measurement, Rhodamine B (Sigma-Aldrich

11   R6626) was used.

12   Fabrication of microchannels: The flexible and PDMS microchannel were fabricated

13   by cutting the channel directly with versalaser cutting engraving system (GCC, Spirit

14   SI-25), at the power of 50 W and cutting speed of 10 mm s^{-1}. The resolution of this

15   system is 1500 PPI. The flexible 3D microchannels had two layers. We made structures

16   both inside the two layers of the VHB tapes, then adhered them together to fabricate 3D

17   microchannels as shown in Figure 1a.

18   Mechanical testing: The EM and PDMS microchannels maintained consistent

19   properties over the time of the tests. All microfluidic devices were prepared with 1.5

20   cm in width, 2.5 cm in length and 2 mm in thickness. The size of channels was ~250 μm

in width, and ~400 μm in height. A homemade device was used to test the stretching

ability of both EM and PDMS elastomers as shown in Figure 2. Screw tightened bars

were utilized to stabilize both ends of samples. Constant tension of the sample could be

finely controlled by the device. All tests were performed in ambient air at room

temperature.

Strain gauge: After we prepared the flexible microchannel pattern with 2 cm in length,

1.5 cm in width, and 2 mm in thickness following the abovementioned method, the

microchannel was filled with 0.1 M KCl as the ionic conductor. The current was

measured while inserting two Ag/AgCl electrodes into the inlet and outlet of the clip. A

voltage of 0.1 V was applied by Keithley 2400 source meter. The sensing test was

performed by stretching from relaxing length of 2 cm to 5.5 cm.

Pressure measurements: A syringe pump was used to supply continuous fluid at a

constant flow rate Q (300 mL min^{-1}) in a single-channeled microfluidics with ~250 μm

in width, and ~400 μm in height. A digital cantilever capable of supplying small amount

of force was harnessed to exert force to the upside surface of the microchannel. A

pressure gauge, pressure transmitter (PX273-030DI) from Omega, connected near the

inlet and outlet of the channel was used to monitor the real-time pressure change, during

flow of deionized water as shown in Figure 4.

Peeling test: All substrates were prepared with 2 cm in width, 3 cm in length and 1 mm

in thickness. The EM was adhered onto various substrates. The samples were tested

1   with a constant 90°-peeling (Instron 5948 microtester) speed of 10 mm min^{-1}. Steady

2   state of peeling force was finally measured in this process.

3   Liquid-leakage critical pressure measurement: The critical pressure was measured

4   following the method mentioned in the pressure measurements section. The size of

5   channels was ~270 μm in width, and ~500 μm in height.

6   Contact angle measurements: The contact angle was measured with a contact angle

7   measurement system (OCA100, Dataphysics) at room temperature. A droplet of 5 μL,

8   either water or dimethylsilicone oil, was placed on the surface of the sample and the

9   droplet profile was captured. For each sample, a mean value of the contact angle was

10   calculated from at least three individual measurements taken at different locations on

11   the examined samples.

12   Surface modification for anti-fouling: The microchannel was modified by PFTS to

13   obtain the anti-fouling capacity. The size of channels is ~250 μm in width, and ~400

14   μm in height. The exposed microchannel inner surface without any treatment was

15   placed in a desiccator together with an open glass dish containing about 0.5 mL of PFTS.

16   Subsequently, the desiccator was closed again and chemical vapor deposition of silane

17   was carried out for 3 h under 80°C. The inner surfaces finally achieved the anti-fouling

18   capacity, and then the two pieces of modified the EM were adhered to form the

19   microfluidic channel. For comparison, an unmodified microfluidic device was also

20   prepared, and these two microfluidic devices were both injected with the Rhodamine B

1   aqueous solution. The Rhodamine B aqueous solution used in the microfluidic

2   experiments was prepared by dissolving Rhodamine B in DI water to give a final

3   concentration of 0.1 mg mL^{-1}. After injecting the Rhodamine B solution into the

4   unmodified/modified microfluidic for 5 second, DI water was injected to wash the

5   channels for 30 seconds. During this process, optical microscopy (Leica, DM6000B)

6   was used to observed the fluorescence.

7

8   ***Supporting Information***

9   Supporting Information is available from the Wiley Online Library or from the author.

10

3

Conflict of Interest

5 *The authors declare no conflict of interest.*

References

7 [1] X. Hou, Y. S. Zhang, G. Trujillo-de Santiago, M. M. Alvarez, J. Ribas, S. J. Jonas,
8   P. S. Weiss, A. M. Andrews, J. Aizenberg, A. Khademhosseini, *Nature Reviews*
9   *Materials* **2017**, *2*, 17016.

10 [2] E. K. Sackmann, A. L. Fulton, D. J. Beebe, *Nature* **2014**, *507*, 181.

11 [3] J. Clayton, *Nat. Methods* **2005**, *2*, 621.

12 [4] D. Psaltis, S. R. Quake, C. Yang, *Nature* **2006**, *442*, 381.

13 [5] T. A. Duncombe, A. M. Tentori, A. E. Herr, *Nature reviews Molecular Cell Biology*
14   **2015**, *16*, 554.

15 [6] G. M. Whitesides, *Nature* **2006**, *442*, 368.

16 [7] Y. Xu, M. Shinomiya, A. Harada, *Adv. Mater.* **2016**, *28*, 2209.

17 [8] B. Xiong, K. Ren, Y. Shu, Y. Chen, B. Shen, H. Wu, *Adv. Mater.* **2014**, *26*, 5525.

18 [9] D. Kim, X. Wu, A. T. Young, C. L. Haynes, *Acc. Chem. Res.* **2014**, *47*, 1165.

19 [10] Y. Cheng, F. Zheng, J. Lu, L. Shang, Z. Xie, Y. Zhao, Y. Chen, Z. Gu, *Adv. Mater.*
20   **2014**, *26*, 5184.

21 [11] Y. S. Zhang, A. Khademhosseini, *Science* **2017**, *356*, 3627.

22 [12] S. Cheng, Y. Jin, N. Wang, F. Cao, W. Zhang, W. Bai, W. Zheng, X. Jiang, *Adv.*
23   *Mater.* **2017**, 29, 1700171.

24 [13] S. Xiao, J. R. Coppeta, H. B. Rogers, B. C. Isenberg, J. Zhu, S. A. Olalekan, K. E.
25   McKinnon, D. Dokic, A. S. Rashedi, D. J. Haisenleder, *Nat. Commun.* **2017**, *8*,
26   14584

27 [14] R. C. R. Wootton, A. J. Demello, *Nature* **2012**, *483*, 43.

28 [15] A. Albanese, A. K. Lam, E. A. Sykes, J. V. Rocheleau, W. C. W. Chan, *Nat.*
29   *Commun.* **2013**, *4*, 2718.

30 [16] P. M. Valencia, O. C. Farokhzad, R. Karnik, R. Langer, *Nature Nanotech.* **2012**, *7*,
31   623.

32 [17] P. Mitchell, *Nat. Biotechnol.* **2001**, *19*, 717.

[18] P. Yager, T. Edwards, E. Fu, K. Helton, K. Nelson, M. R. Tam, B. H. Weigl, *Nature* **2006**, *442*, 412.

[19] M. Kaltenbrunner, T. Sekitani, J. Reeder, T. Yokota, K. Kuribara, T. Tokuhara, M. Drack, R. Schwödiauer, I. Graz, S. Bauer-Gogonea, *Nature* **2013**, *499*, 458.

[20] S. Xu, Y. Zhang, L. Jia, K. E. Mathewson, K. I. Jang, J. Kim, H. Fu, X. Huang, P. Chava, R. Wang, *Science* **2014**, *344*, 70.

[21] J. C. Yeo, J. Yu, K. P. Loh, Z. Wang, C. T. Lim, *ACS Sensors* **2016**, *1*, 543.

[22] X. Pu, M. Liu, X. Chen, J. Sun, C. Du, Y. Zhang, J. Zhai, W. Hu, Z. Wang, *Sci. Adv.*, **2017**, 3, e1700015.

[23] A. Chortos, J. Liu, Z. Bao, *Nature Mater.* **2016**, *15*, 937.

[24] J. Kim, M. Lee, H. J. Shim, R. Ghaffari, H. R. Cho, D. Son, Y. H. Jung, S. Min, C. Choi, S. Jung, *Nat. Commun.* **2014**, *5*, 5747.

[25] D. Qin, Y. Xia, G. M. Whitesides, *Nat. Protoc.* **2010**, *5*, 491.

[26] M. K. Verma, A. Majumder, A. Ghatak, *Langmuir.* **2006**, *22*, 10291.

[27] H. Ota, K. Chen, Y. Lin, D. Kiriya, H. Shiraki, Z. Yu, T. J. Ha, A. Javey, *Nat. Commun.* **2014**, *5*, 5032.

[28] D. Ziegler, T. Suzuki, S. Takeuchi, *J. Microelectromech. Syst.* **2006**, *15*, 1477.

[29] S. Metz, R. Holzer, P. Renaud, *Lab on a chip* **2001**, *1*, 29.

[30] R. Mukhopadhyay, *Anal. Chem.* **2005**, *77*, 429.

[31] K. J. Regehr, M. Domenech, J. T. Koepsel, K. C. Carver, S. J. Ellison-Zelski, W. L. Murphy, L. A. Schuler, E. T. Alarid, D. J. Beebe, *Lab on a chip* **2009**, *9*, 2132.

[32] S. Marre, Y. Roig, C. Aymonier, *J. Supercrit. Fluid.* **2012**, *66*, 251.

[33] N. Kockmann, J. Kastner, P. Woias, *Chem. Eng. J.* **2008**, *135*, S110.

[34] H. Yuk, Z. Teng, G. A. Parada, X. Liu, X. Zhao, *Nat. Commun.* **2016**, *7*, 12028.

[35] M. Kubo, X. Li, C. Kim, M. Hashimoto, B. J. Wiley, D. Ham, G. M. Whitesides, *Adv. Mater.* **2010**, *22*, 2749.

[36] S. A. Morin, G. M. Whitesides, *Science* **2012**, *337*, 828.

[37] I. Wagner, E. M. Materne, S. Brincker, U. Süssbier, C. Frädrich, M. Busek, F. Sonntag, D. A. Sakharov, E. V. Trushkin, A. G. Tonevitsky, *Lab on a chip* **2013**, *13*, 3538.

[38] D. Snakenborg, H. Klank, J. P. Kutter, J. Micromech. *Microeng.* **2003**, 14, 182.

[39] F. Cortés-Salazar, M. Träuble, F. Li, J. M. Busnel, A. L. Gassner, M. Hojeij, G. Wittstock, H. H. Girault, *Anal. Chem.* **2009**, *81*, 6889.

[40] J. R. Anderson, D. T. Chiu, H. Wu, O. Schueller, G. M. Whitesides, *Electrophoresis* **2000**, *21*, 27.

[41] K. Ren, W. Dai, J. Zhou, J. Su, H. Wu, *Proc. Natl. Acad. Sci. USA.* **2011**, *108*, 8162.

[42] A. C. Burton, *Am. J. Physiol.* **1951**, *164*, 319.

[43] W. Wu, A. Deconinck, J. A. Lewis, *Adv. Mater.* **2011**, *23*, 178.

[44] B. Yuan, Y. Jin, Y. Sun, D. Wang, J. Sun, Z. Wang, W. Zhang, X. Jiang, *Adv. Mater.* **2012**, *24*, 890.

[45] P. Gong, W. Zheng, Z. Huang, W. Zhang, D. Xiao, X. Jiang, *Adv. Funct. Mater.* **2013**, *23*, 42.

[46] J. Lee, J. Wu, M. Shi, J. Yoon, S. Park, M. Li, Z. Liu, Y. Huang, J. A. Rogers, *Adv. Mater.* **2011**, *23*, 986.

[47] Y. Su, X. Ping, K. J. Yu, J. W. Lee, J. A. Fan, B. Wang, M. Li, R. Li, D. V. Harburg, Y. Huang, *Adv. Mater.* **2017**, *29*, 1604989.

[48] K. Ren, Y. Chen, H. Wu, *Curr. Opin. Chem. Biol.* **2014**, *25*, 78.

[49] P. L. Floch, X. Yao, Q. Liu, Z. Wang, G. Nian, Y. Sun, L. Jia , Z. Suo, *ACS Appl. Mat. Interfaces*, **2017**, DOI: 10.1021/acsami.7b07361.

[50] C. J. Morris, F. K. Forster, *Exp. Fluids.* **2004**, *36*, 928.

[51] M. J. Fuerstman, A. Lai, M. E. Thurlow, S. S. Shevkoplyas, H. A. Stone, G. M. Whitesides, *Lab on a chip* **2007**, *7*, 1479.

[52] M. Y. Liu, H. Wang, Y. Wang, *Aiche. J.* **2010**, *53*, 1075.

[53] Andrea R. Statz, Robert J. Meagher, a. Annelise E. Barron, Phillip B. Messersmith, *J. Am. Chem. Soc.* **2005**, *127*, 7972.

1 **Supporting Information**

2

3 Bioinspired Universal Flexible Elastomer-Based Microchannels

4 *Feng Wu, Songyue Chen, Baiyi Chen, Miao Wang, Lingli Min, Jack Alvarenga, Jie Ju, Ali Khademhosseini,*

5 *Yuxing Yao, Yu Shrike Zhang, Joanna Aizenberg, and Xu Hou*[*]

6

7 F. Wu, Dr. M. Wang, Prof. X. Hou

8 Bionic and Soft Matter Research Institute, College of Physical Science and Technology

9 Xiamen University

10 361005, Xiamen, China

11 E-mail: houx@xmu.edu.cn

12 Prof. S. Chen

13 Department of Mechanical and Electrical Engineering

14 Xiamen University

15 361005, Xiamen, China

16 Dr. B. Chen, Dr. L. Min, Prof. X. Hou

17 College of Chemistry and Chemical Engineering, and Collaborative Innovation Center of Chemistry for Energy

18 Materials, and State Key Laboratory of Physical Chemistry of Solid Surfaces, and Pen-Tung Sah Institute of Micro-

19 Nano Science and Technology

20 Xiamen University

21 361005, Xiamen, China

22 Dr. J. Alvarenga, Dr. Y. S. Zhang, Prof. A. Khademhosseini, Prof. J. Aizenberg

23 Wyss Institute for Biologically Inspired Engineering

24 Harvard University

25 MA 02138, Cambridge, USA

26 Dr. J. Ju, Dr. Y. S. Zhang, Prof. A. Khademhosseini

27 Biomaterials Innovation Research Center, Division of Engineering in Medicine, Department of Medicine, Brigham

28 and Women's Hospital

29 Harvard Medical School

30 MA 02139, Cambridge, USA

31 Y. Yao, Prof. J. Aizenberg

32 Department of Chemistry & Chemical Biology

33 Harvard University

34 MA 02138, Cambridge, USA

35

36

37

38

39

40

1   For 3D microchannels (Video S1, Supporting Information), there were

2   discontinuous microchannels that we specially designed to test the sealability of the

3   microfluidics. The discontinuously microchannels would block the liquid flow during

4   stretching and releasing state that showed the excellent sealing.

5   The channels could be homogeneously fabricated (Figure S1 and S2, Supporting

6   Information). Meanwhile, this method was also applicable for the microchannel sizes

7   down to the sub-micron scale (Figure S2, Supporting Information).
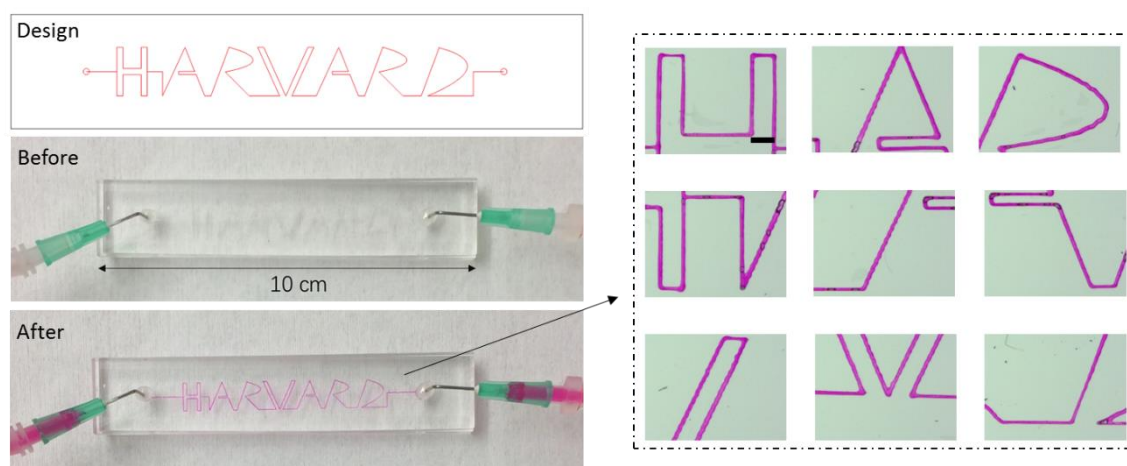
8   **Figure S1.** The pattern "HARVARD" of microchannel was designed to prepare the 2D microchannel (Left). More
9   details about the microchannel were shown on the right. Scale bar, 1 mm.
10
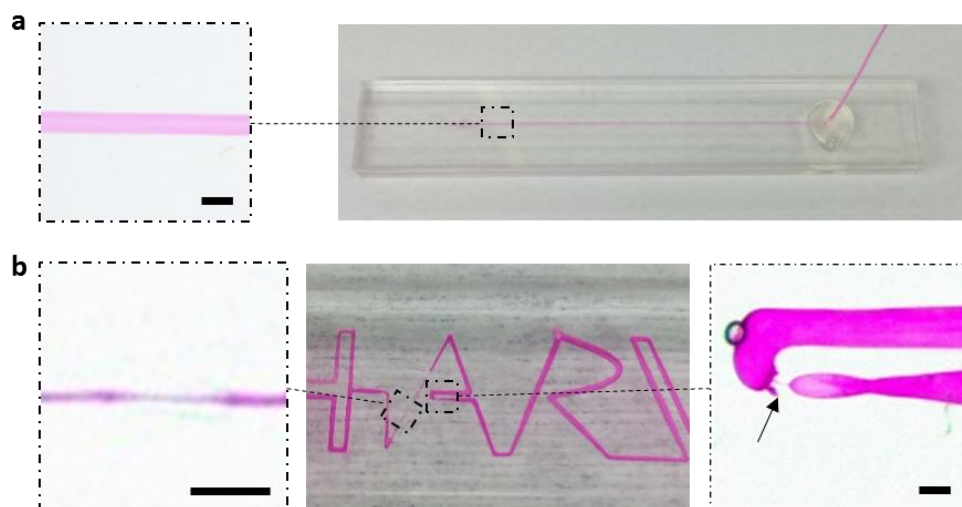
11

Figure S2. a) The homogeneous microchannel. b) The channel was fabricated with the size of tens of micrometers down to sub-micron. Scale bars, 200 μm.

The channel dimensions could be controlled by the laser power and the engraving time. In this work, we studied the impact of engraving speed on the size of the channels at the power of 50 W. Table S1 and Figure S3 indicate that the lower cutting speeds would increase the channel sizes, while higher cutting power would accumulate on the substrate at a slower speed. It is worth noting that the laser would pass through the EM at speed of less than 3 mm/s. The smallest size of channel fabricated by the laser cutting system was ~200 μm due to the limitation of the spot size of the versalaser cutting system, which was above 70 μm.
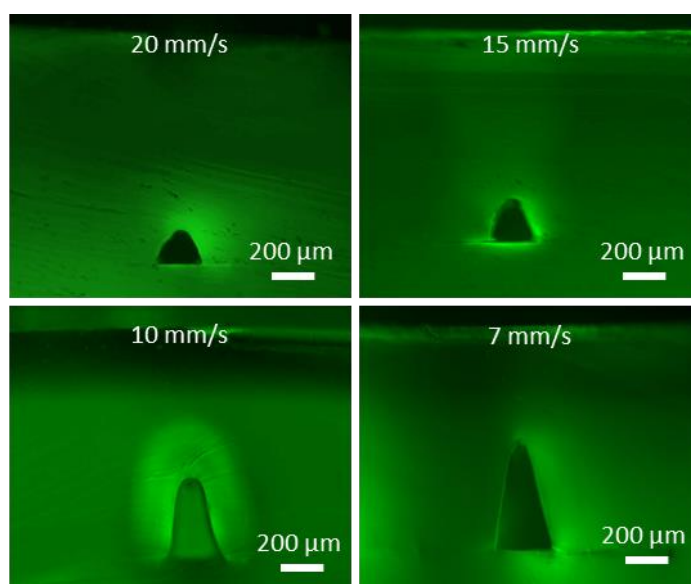
Table S1. Different sizes of the microchannel prepared at the different engraving speeds.

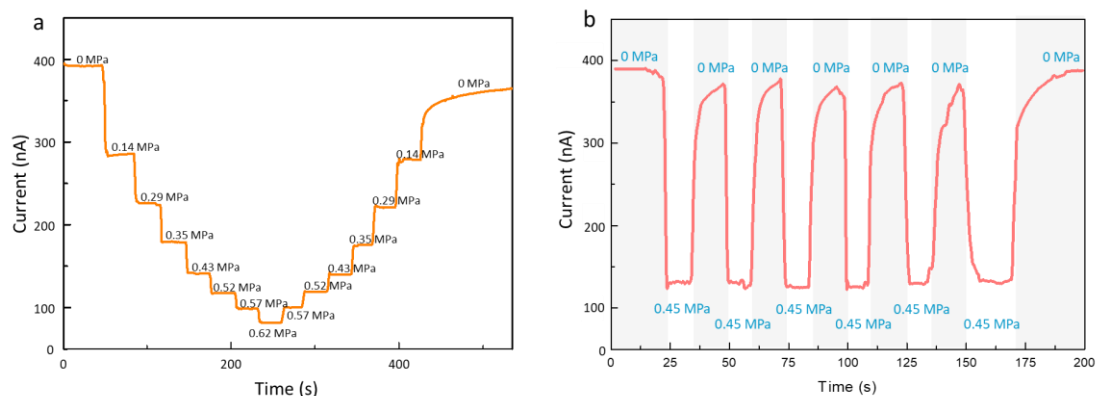| Engraving speed (mm/s)	20	15	10	7
Height (μm)	151.38	189.17	392.85	510.37
Width (μm)	207.14	224.05	254.58	278.73

Figure S3. The cross-section of elastomer-based microchannel fabricated at the different engraving speeds.

The force sensor remained stable after being stretched 2 times of the original length for 10 s; then it was released completely and maintains for 15 s.

Figure S4. a) The real-time strain gauge testing by stretching and releasing the elastomer-based microchannel. The current was measured with the stretching EM at 0.5 cm per interval. The value of the forces is shown above the curve. b) Current changes under repeated the stretch and release from 0% to 100% for the cycles test.

To measure the adhesion between EM and various substrates, we used the 90°-peeling test and the liquid-leakage critical pressure measurement, as shown in Figure S5. The peeling force (Figure S5a-c, Supporting Information) was consistent with the liquid-leakage critical pressure (Figure S5d, Supporting Information) in the order Metal-EM > Glass-EM > PET-EM > PMMA-EM > PDMS-EM > PTFE-EM. This similarity could be explained by the surface energy or surface roughness. Overall, the liquid-leakage critical pressure was more than the liquid-leakage critical pressure (~3.3 MPa), exhibiting the good sealing property.
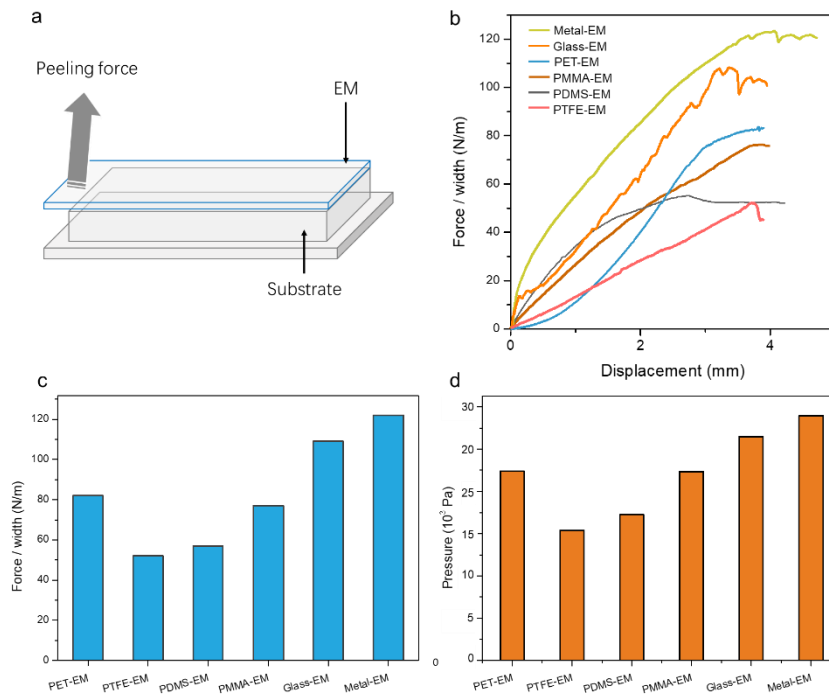
Figure S5. a-c) The 90°-peeling test between the EM and various substrates. d) The liquid-leakage critical pressure between the EM and various substrates.